Journal of
MATERIALS RESEARCH

Synthesis of cobalt oxide nanocrystal self-assembled materials

J. S. Yin and Z. L. Wang[a)]
School of Materials Science and Engineering, Georgia Institute of Technology, Atlanta, Georgia 30332-0245

(Received 12 August 1997; accepted 3 May 1998)

Self-assembling of size, shape, and phase-selected nanocrystals into superlattices in a new approach for synthesizing a new generation of advanced materials with functionality. In this paper, high purity and monodispersive tetrahedral of CoO, with edge lengths of 4.4 ± 0.2 nm, have been synthesized and separated from Co nanocrystals using colloidal chemistry and magnetic separation. The tetrahedral CoO nanocrystals behave like a molecular matter, and their assembling forms superlattices with translational symmetry. The phase transformation of the CoO nanocrystals is examined by *ex situ* annealing in oxygen, and the results showed the formation of Co_3O_4 with spinel structure.

I. INTRODUCTION

Nanocrystal materials have many potential applications owing to their unique particle sizes and surface effects.[1–10] Very recently, there has been a great deal of interest in making monodispersive nanocrystals and assembling these nanocrystals into well-organized two- and three-dimensional "quantum" crystals. The quantum crystals can be used in data storage, solar absorber, optical gratings, and other microelectronics devices. In addition to the fascinating properties offered by the nanocrystals themselves, one unique advantage of the quantum crystals is the flexibility of controlling the interparticle distance, allowing tunable interparticle interaction and coupling properties. The size of the nanocrystals is controlled to be smaller than 10 nm, below which the quantum effect is significant. Up to now *self-assembly passivated nanocrystal superlattices (NCS's) or nanocrystals arrays (NCA)* have been successfully fabricated using metal,[11–16] semiconductor,[17–19] oxide,[20] and sulfite[21] clusters. Well-defined ordered solids prepared from tailored nanocrystalline building blocks provide new opportunities for optimizing and enhancing the properties and performance of the materials. This is a new initiative of research on *cluster engineered materials.*

There are two key components for constructing the NCS's. First, the nanocrystal cores are required to be monodispersive, even with controlled shape. Second, the surface passivation molecules need to be chemically active to cap tightly on the surfaces of the nanocrystals. This surface-coating layer separates, protects, and links the nanocrystal cores, forming ordered superlattices with translation and even orientational order. The length and density of the surface-passivated molecules as well as the size of the nanocrystals cores determine the crystallography of the three-dimensional packing. The length of the molecules can be easily optimized by choosing different carbon chains; thus, the two- and three-dimensional cluster self-assembled superlattice structures in fact are well-organized inorganic-organic composites.[22]

Processing of size- and even shape-controlled nanocrystal molecules at high purity and large quantity is the key. In most of the current reports on NCS's, the size of the nanocrystals is precisely controlled, while the particle shape is dominated by spherical or spherical-like except the Ag NCS reported by Harfenist *et al.*[15] In the current paper, we report the preparation of self-assembled NCS's of CoO nanocrystals with a tetrahedral shape. Details of the experimental procedures are given in Sec. II. The structures of the NCS's are analyzed in Sec. III. The shape and structural transformation behavior of the CoO nanocrystals will also be examined (Sec. IV).

II. EXPERIMENTAL METHOD

Colloidal chemistry is a powerful approach for synthesis of size- and even shape-controlled nanocrystals. Cobalt and cobalt oxide nanocrystals were processed by chemical decomposition of $Co_2(CO)_8$ in toluene.[23–25] homogeneous nucleation and growth must be maintained to grow monodispersive nanocrystals. The temperature should be kept uniform but not too high since the melting point of the organic molecules is low. To avoid agglomeration of the freshly nucleated nanocrystals, sodium bis(2-ethylhexyl) sulfosuccinate [$C_{20}H_{37}O_2SNa$, in short Na(AOT)] was added as a surface active agent at the beginning of the growth, forming a monolayer passivation (called sulfate) over the nanocrystal surface. The sulfate serves not only as the protection layer for the particles to avoid direct contact between the particles, but also the interparticle bonding. Typically, 100 mg of $Co_2(CO)_8$ and 50 mg of Na(AOT) were dispersed

[a)]Address all correspondence to this author.
e-mail: zhong.wang@mse.gatech.edu

into 25 ml of toluene at room temperature, then the mixed solution was ultrasonically dispersed and heated at 130 °C for 4 h in air. This temperature was chosen to ensure the crystallinity of the nanocrystals. By adjusting the wt. % ratio between the precursor and Na(AOT) from 1 : 1 to 5 : 1, the particle size was controlled to be smaller than 5 nm. Then the mixed solution was diluted to 1 : 4 by adding more toluene.

The as-prepared solution contained Co, CoO, and possibly Co_3O_4 particles. A size selection was required to obtain pure molecular nanocrystals with specific size and even shape. Since Co particles are superparamagnetic when their sizes are smaller than 10 nm, while CoO is antiferromagnetic, a small magnetic field, generated by a horse-shoe permanent magnet, was applied in the vertical direction (with the **N** pole at the top), so that the Co nanoparticles floated to the top surface of the liquid under the driving force of the magnetic field, forming aggregates, while the CoO particles were left in the solution. Though there is gravity force, the smaller size particles can still suspend in the liquid because of the Brown motion, while the larger ones sank to the bottom. By picking the particles suspended at different depths of the solution after 24 h in the magnetic field, the size- and phase-selected CoO nanoparticles were obtained.

The structure of the nanocrystals was determined using transmission electron microscopy (TEM). For TEM observations, a drop of solution was deposited on a ultrathin carbon or SiO film supported by a copper grid and dried in air naturally. The TEM experiments, including bright-field (BF) image, dark-field (DF) image, selected diffraction pattern, the energy dispersive x-ray spectroscopy (EDS), and the electron energy loss spectrum (EELS) were performed at 200 kV using a Hitachi HF-2000 TEM equipped with a field emission source.

III. SELF-ASSEMBLING OF NANOCRYSTALS

As a start of our analysis, the collective property of the CoO nanocrystals in solution is examined by light absorption, as shown in Fig. 1. Two characteristics are observed. First, an abrupt change in optical density occurs within 0.1 eV, indicating the distribution in band gap energies is very narrow; thus, the distribution of particle sizes is narrow for the following reason. From the solid state theory, the band gap for nanoparticles is directly associated with the size of the particles, and it is expected that the band gap becomes wider as the particles are smaller.[26,27] Second, the average band gap of the nanocrystals is about 4.45 eV, which is dramatically larger than 4.0 eV, the band gap of bulk CoO. This study clearly indicates that our synthesis and size separation technique can produce a large quantity of narrow size distribution CoO nanocrystals.

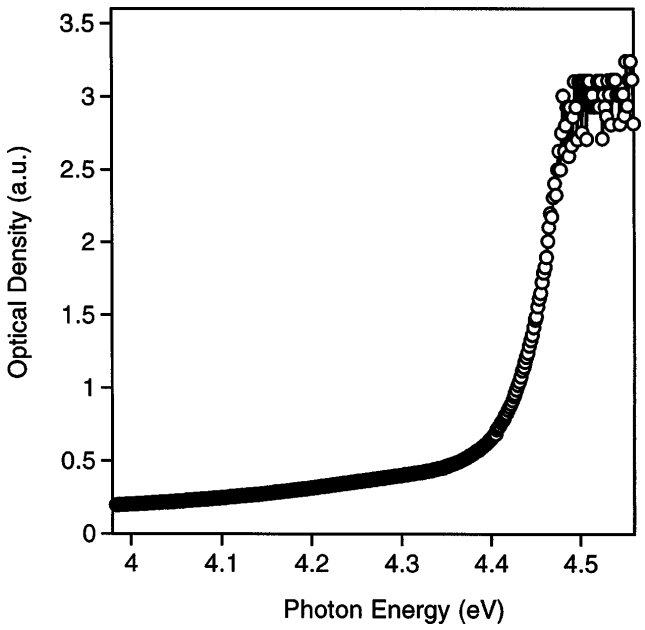

FIG. 1. Light absorption spectrum of colloidal CoO nanocrystals suspended in toluene.

Self-assembling of the prepared nanocrystals is a natural process during the drying of the liquid supported by a carbon/SiO film. An BF TEM image is shown in Fig. 2, from which the monodispersity of the nanocrystals is clearly presented. The particles are assembled into monolayers and more than 90% of the particles have sizes in the range of 4–5 nm. It is interesting to note that most of the particles exhibit triangle contrast in the image, simply indicating that the particle shape is nonspherical. An electron diffraction pattern recorded from the specimen indicates that the structure is cubic and it can be indexed as face-centered cubic. EDS and EELS analysis indicated the presence of Co and O in the specimen; thus, the nanocrystals are CoO with the NaCl structure. This structure was confirmed by the EELS measurement of Co valence.[28] Co_3O_4 has the spinel structure ($a = 8.083$ Å) and Co is face-centered-cubic (*fcc*) ($a = 3.548$ Å), but the lattice constants of both are significantly different from that of CoO ($a = 4.2667$ Å). Quantitative analysis of the electron diffraction pattern in reference to a standard pattern recorded from an aluminum polycrystalline thin film under the same conditions proves the CoO structure.

The size selected CoO nanocrystals behave like molecules, forming monolayer and multilayer self-assembling arrays [Fig. 3(a)]. Translation symmetry is evident in local regions, although the entire image shows largely disordered structure. The array can be viewed as thin films comprised of orderly distributed nanocrystals, in which each nanocrystal is a building block, the unit cell of the packing is the superlattice. The particle

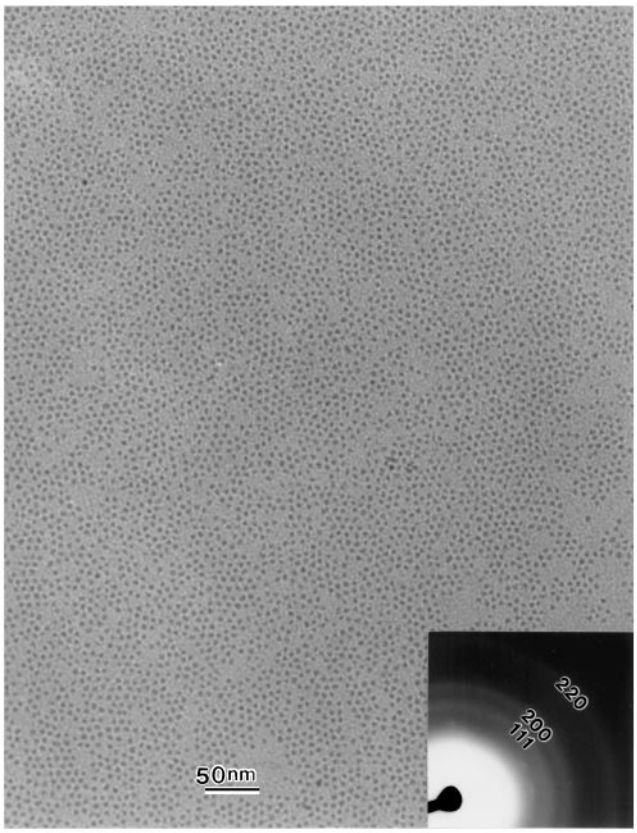

FIG. 2. A bright-field TEM image of CoO nanocrystals, passivated with Na(AOT) and dispersed on a carbon film, showing monodispersity and self-assembling. The image was recorded at 200 kV using a Hitachi HF-2000 field emission TEM. The inset is an electron diffraction pattern recorded from a large area of the assembled nanocrystals. Using the Al polycrystalline as a standard, the crystal structure is identified to be CoO.

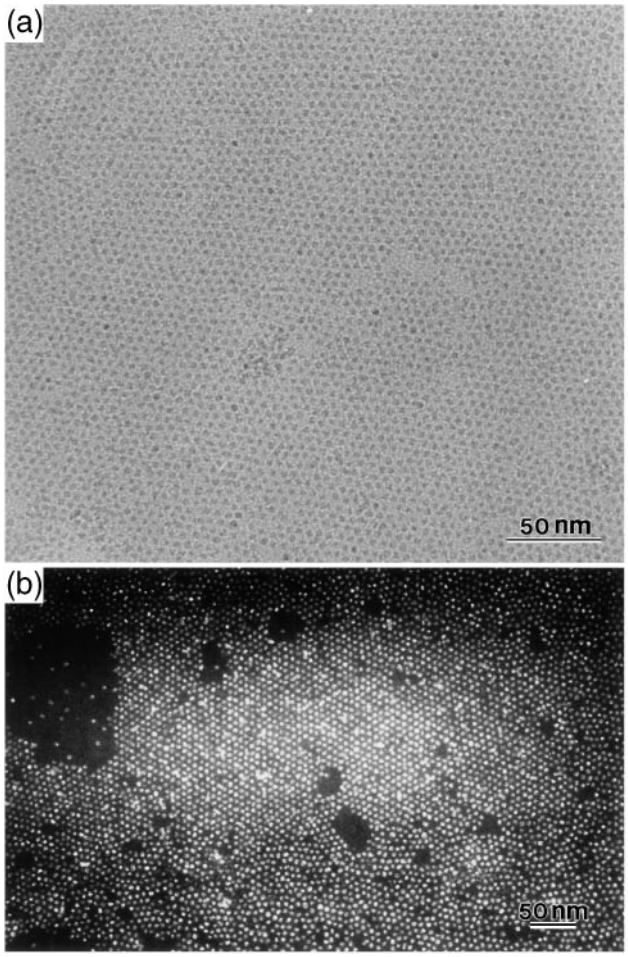

FIG. 3. (a) A bright-field TEM image of CoO nanocrystals, showing the formation of ordered superlattice packing with translational order. It is apparent that the projected shapes of the nanocrystals are dominated by triangles, indicating the monodispersive tetrahedral shape. (b) Dark-field TEM image showing monolayer and multilayer packing as judged from the image contrast. A careful examination of the particles at the monolayer assembling region shows nonuniform contrast across each nanocrystal, in support of the tetrahedral shape derived from BF TEM images.

contrast is rather weak in the BF TEM images due to the presence of carbon support and the sulfate layer. To increase the contrast, DF TEM images are recorded to differentiate the regions packed into multilayers from the ones of monolayers. By selecting the electrons falling into a specific angular range, as defined by the position and size of the objective aperture, one may find the real space distribution of the particles which are oriented in directions that give the Bragg reflections falling in the selected angular range. Figure 3(b) is an DF TEM image of the synthesized CoO nanocrystals recorded using a rather large objective aperture, displaying regions with a monolayer assembling of nanocrystals and regions with double layer packing. The nonuniform contrast of the nanocrystals is due to a distortion in their orientational order. The ordered structure of the superlattice is evident in the image.

From the BF TEM images recorded at near in-focus condition [Fig. 3(a)], the nanocrystals apparently show triangle projected shapes. More than 53% of the nanocrystals with recognizable shapes can be attributed to triangles, 10% are irregular shapes, and 27% are cubic and spherical-like. There are two possible geometrical configurations that are likely to give the projected triangular shapes in the nanocrystal system: one is a tetrahedron bounded by four {111} facets, and the other is a (111) based platelet structure. If the latter was the structure seen here, the contrast of the nanocrystals in the dark-field image would be uniform because of the uniform thickness of the nanocrystal. In contrast, the experimental image shown in Fig. 3(b) indicates that, in the region with monolayer assembling, the contrast across each nanocrystal is nonuniform, rather there is a white dot in the image of each nanocrystal, suggesting that the nanocrystals have a tetrahedral shape and the white dot corresponds to the projected position of the vertical apex of the tetrahedron. The tetrahedral shape

of the nanocrystals has also been confirmed by high-resolution TEM.[28]

IV. PHASE TRANSFORMATION INDUCED BY ANNEALING IN OXYGEN

The stability and phase transformation behavior of nanocrystals is an important issue because of their small sizes. To examine this behavior, self-assembling CoO nanocrystals onto a carbon film were annealed at 250 °C in oxygen for 18 h. Figure 4(a) is an BF TEM image of the nanocrystals after thermal treatment. The particle shapes become unclear and the local aggregation is visible. To determine the phase formed after the *ex situ* experiment, an electron diffraction pattern was recorded from the nanocrystals [Fig. 4(b)]. This pattern is distinctly different from the one shown in Fig. 2. To precisely index the pattern, a diffraction pattern was recorded from a standard Co_3O_4 polycrystalline specimen. The diffraction rings observed in the standard pattern correspond well to the ones shown in Fig. 4(b) except the inner most ring, due to the strong background generated from the scattering of the amorphous carbon substrate. Therefore, it is obvious that the CoO nanocrystals had been transformed into Co_3O_4 after an annealing in oxygen. Another distinctive feature is that the packing of monolayer has been changed into separated particle agglomerations, and the shapes of the particles are irregular although a small portion of the particles still preserve the tetrahedral shape.

V. DISCUSSION

A. Surface passivation and stability of tetrahedral nanocrystals

Tetrahedral nanocrystals have been observed in several nanocrystal systems, such as CdSe[29] and Pt,[30] in which the bonds are covalent or metallic, respectively; thus, no ionic charge balance is needed. For CoO with ionic bonds, however, the charge balance is a key factor in determining the crystal shape and surface structure. The most stable shape for NaCl-type structure with ionic bonds may be cubic [Fig. 5(a)], in which the total number of cations equals to that of anions. A tetrahedral particle is formed by cutting off four corners of the cube, exposing four {111} planes [Fig. 5(b)]. The {111} surfaces are terminated with either all cations or all anions; thus the surface has a net charge, different from the {100} surfaces. For this ideal tetrahedron, if the number of cation layers (assumed to be the gray balls located at the outer most surface layer) along each edge is n and the corresponding number of anion layers is $n - 2$, the number of cations and anions in the tetra-

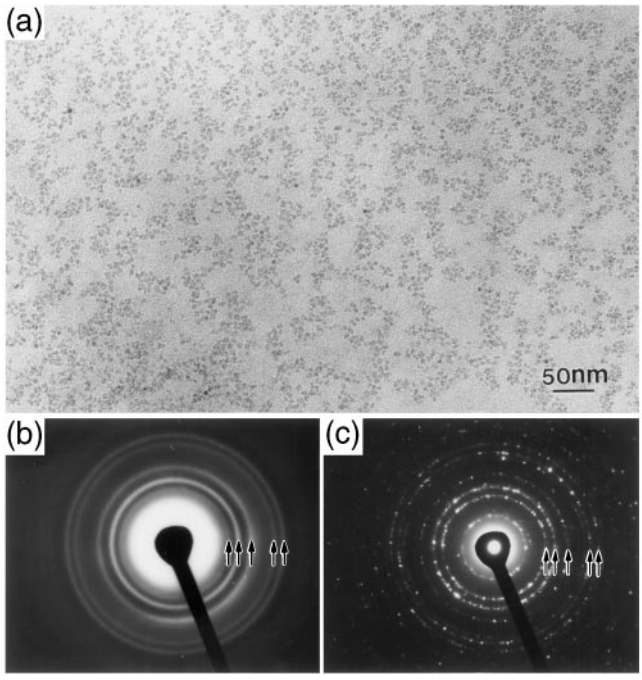

FIG. 4. (a) Bright-field TEM images of CoO nanocrystals after treatment in oxygen at 250 °C for 18 h, showing the destroying of the self-assembling. (b) Electron diffraction pattern of the nanocrystals after heat treatment, showing a distinct difference from the inset in Fig. 2. (c) Electron diffraction pattern from a standard powder sample of Co_3O_4.

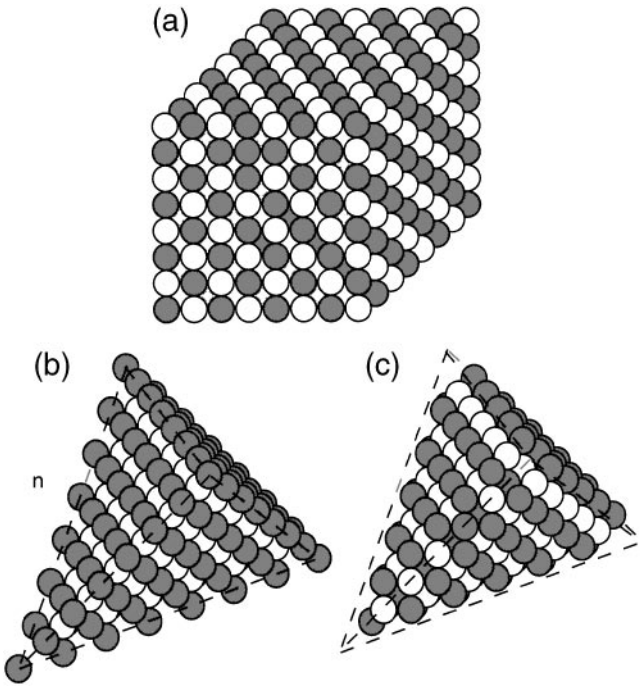

FIG. 5. (a) An ideal cubic shape CoO nanocrystal with neutral charge. (b) An ideal tetrahedral shape CoO nanocrystal with unbalanced charge. The model shown here is for a case with $n = 8$. (c) A truncated tetrahedral CoO nanocrystal after removing the atoms at the edges and apexes but still with unbalanced charge.

hedron are, respectively,

$$N_c = \sum_{i=1}^{n} \frac{i(i+1)}{2} = \frac{1}{6} n(n+1)(n+2),$$

and

$$N_a = \sum_{i=1}^{n-2} \frac{i(i+1)}{2} = \frac{1}{6} (n-2)(n-1)n.$$

The number of cation atoms on the edges including the apexes is $N_e = 6n - 8$. The number of atoms on the surface including the edges and apexes is

$$N_s = 4 \sum_{i=1}^{n-3} i + 6n - 8 = 2(n-3)(n-2) + 6n - 8.$$

The anion coordination number for each cation at the edge is 2 and is zero for the cation at the apex; thus, an ideal tetrahedron is very unstable and the atoms at the edges and apexes are likely to be repelled, resulting in the formation of a truncated tetrahedron (TT) as shown in Fig. 5(c). In this model, the total number of anions is preserved, while the total number of cations reduces into

$$N_c' = N_c - N_e = \frac{1}{6} n(n+1)(n+2) - 6n + 8.$$

Disregarding the surface energy, the first condition for an uncapped TT nanocrystal to be stable is the charge balance, i.e., $N_a = N_c'$, which is possible only for $n = 4$, corresponding to a cluster with 4 cations and 4 anions. This type of cluster, if it exists, is hardly seen using high-resolution TEM.

Based on the fundamental cubic NaCl lattice, a cubic shape particle is energetically favorable, such as the MgO cubes. This is the case of free particle growth of MgO smokes while burning Mg ribbons in air. For a freestanding TT CoO particle, the entire structure is likely unstable regardless of the surface atoms being either Co or O, simply because of unbalance charge unless high density of point defects exist. Therefore, it is speculated that the long-chain molecules must have played a vital role in the formation of the tetrahedral nanocrystals. As we pointed out earlier, the concentration of the organic molecules is the key to control the monodispersity and particle sizes.

Nanoclusters of tetrahedral shape have been observed in the Cd–S system.[31–33] The nucleation and growth mechanism of the tetrahedral particles in liquid with the presence of long-chain molecules, however, is a complex process. It is proposed that the replacement and reattachment of the estabilizer could be the process for forming the nanoparticles.[34]

B. Annealing induced structure transformation

The oxidation of the nanocrystals is air was confirmed by the electron diffraction patterns shown in Fig. 4(b). As the temperature increases, the reaction rate of oxygen with CoO and the diffusion rate of oxygen through the passivative Na(AOT) layer are likely to increase, resulting in the oxidation of CoO into Co_3O_4. The transition temperature is rather low due to the small sizes. The preservation of some particle shape may be because the annealing temperature is still low (250 °C). *In situ* annealing of CoO in a vacuum better than 3×10^{-8} Torr has found a shape transformation at temperatures higher than 300 °C.[35]

One interesting phenomenon needed to be mentioned in that, compared with the *in situ* heating experiment of the same kind of sample in TEM,[33] the reactant in *ex situ* experiments is totally different. In both cases it is believed that the organic Na(AOT) was evaporated first before the reaction took place. But in the case of *in situ* experiment without the presence of oxygen, the CoO nanocrystals react with carbon to form cobalt carbides instead of Co_3O_4 simply because of the lack of oxygen in the environment.

VI. CONCLUSIONS

Self-assembling of size, shape, and phase-controlled nanocrystals into superlattices is a new trend for synthesizing high performance smart materials. Self-assembling is performed by packing monodispersive nanocrystals coated with organic molecules into superlattices so that the ordered structure is preserved in two length scales, the atomic dimension and the nanocrystal level. In this paper, high purity and monodispersive tetrahedral nanocrystals of CoO have been synthesized and separated from Co nanocrystals using colloidal chemistry and magnetic separation. The tetrahedral CoO nanocrystals behave like a molecular matter and their assembling forms superlattices with translational symmetry. Finally, structural transformation of CoO nanocrystals is examined by *ex situ* annealing in oxygen, and the results clearly showed the formation of Co_3O_4 with spinel structure.

ACKNOWLEDGMENTS

Thanks to Mr. J. P. Wang and Professor M. A. El-Sayed for providing the optical absorption measurement facility and assistance. This work was supported in part by NSF Grant No. DMR-9632823.

REFERENCES

1. D. J. Wales, Science **271**, 925 (1996), and all the review articles in the Feb. 16 issue of Science (1996).
2. M. A. Kastner, Phys. Today **46** (1), 24 (1993).
3. L. N. Lewis, Chem. Rev. **93**, 2693 (1993).

4. R. Freer, *Nanoceramics* (Institute of Materials, London, 1993).
5. D. D. Awschalom and D. P. DiVincenzo, Phys. Today **48** (4), 43 (1995); J. Shi, S. Gider, K. Babcock, and D. D. Awschalom, Science **271**, 937 (1996).
6. J. F. Smyth, Science **258**, 414 (1992).
7. P. V. Braun, P. Osenar, and S. I. Stupp, Nature (London) **380**, 325 (1996).
8. H. Weller, Angew. Chem. **35**, 1079 (1996).
9. T. S. Ahmadi, Z. L. Wang, T. C. Green, A. Henglein, and M. A. El-Sayed, Science **28**, 1924 (1996).
10. W. D. Luedtke and U. Landman, J. Phys. Chem. B **100**, 13–323 (1996).
11. R. L. Whetten, J. T. Khoury, M. M. Alvarez, S. Murthy, I. Vezmar, Z. L. Wang, C. C. Cleveland, W. D. Luedtke, and U. Landman, Adv. Mater. **8**, 428 (1996).
12. J. Dorogi, J. Gomez, R. Osifchin, R. P. Andres, and R. Refenberger, Phys. Rev. B **52**, 9071 (1995).
13. D. V. Leff, P. C. Ohara, J. R. Heath, and W. M. Gelbart, J. Phys. Chem. **99**, 7036 (1995).
14. R. P. Andres, T. Bein, M. Dorogi, S. Feng, J. I. Henderson, C. P. Kubiak, W. Mahoney, R. G. Osifchin, and R. Reifenberger, Science **273**, 1690 (1996).
15. S. A. Harfenist, Z. L. Wang, M. M. Alvarez, I. Vezmar, and R. L. Whetten, J. Phys. Chem. B **100**, 13 904 (1996); S. A. Harfenist, Z. L. Wang, M. M. Alvarez, I. Vezmar, and R. L. Whetten, Adv. Mater. **9**, 817 (1997).
16. J. R. Heath, C. M. Knobler, and D. V. Leff, J. Phys. Chem. B **101**, 18 (1997).
17. C. B. Murray, C. R. Kagan, and M. G. Bawendi, Science **270**, 1335 (1995), and the references therein.
18. L. Brus, Appl. Phys. A **53**, 465 (1991).
19. A. P. Alivisatos, Science **271**, 933 (1996), and references therein.
20. M. D. Bentzon, J. Van Wonterghem, S. Mørup, A. Thölen, and C. J. W. Koch, Philos. Mag. B **60**, 169 (1989).
21. L. Mott, F. Billoudet, E. Lacaze, and M-P. Pileni, Adv. Mater. **8**, 1018 (1996).
22. S. I. Stupp, V. LeBonheur, K. Walker, L. S. Li, K. E. Huggins, M. Kerser, and A. Amstutz, Science **276**, 384 (1997).
23. J. R. Thomas, J. Appl. Phys. **37**, 2914 (1966).
24. J. P. Chen, C. M. Sorensen, K. J. Klabunde, and G. C. Hadjipanayis, Phys. Rev. B **51** (17), 11 527 (1995).
25. E. Papiper, P. Horny, H. Balard, R. Anthore, C. Petipas, and A. Martinet, J. Colloid Interface Sci. **94** (1), 207 (1983).
26. P. E. Lippens and M. Iannoo, Phys. Rev. B **39**, 10 935 (1989).
27. L. E. Brus, J. Chem. Phys. **79**, 5566 (1983).
28. J. S. Yin and Z. L. Wang, Phys. Rev. Lett. **79** (13), 2570 (1997).
29. A. P. Alivisatos, J. Phys. Chem. **100**, 13226 (1996).
30. T. S. Ahmadi, Z. L. Wang, T. C. Green, A. Henglein, and M. A. El-Sayed, Science **28**, 1924 (1996); Z. L. Wang, T. S. Ahmadi, and M. A. El-Sayed, Surf. Sci. **380**, 302 (1997).
31. N. Herron, J. C. Calabrese, W. E. Farneth, and Y. Wang, Science **259**, 1426 (1993).
32. T. Vossmeyer, G. Reck, L. Katsikas, E. T. K. Haupt, B. Schulz, and H. Weller, Science **267**, 1476 (1995).
33. T. Vossmeyer, G. Reck, B. Schulz, L. Katsikas, and H. Weller, J. Am. Chem. Soc. **117**, 12 881 (1995).
34. Y. Wang and N. Herron, J. Phys. Chem. **95**, 525 (1991).
35. J. S. Yin and Z. L. Wang, J. Phys. Chem. B **101**, 8979 (1997).